Received: 12 October 2024 | Revised: 13 January 2025 | Accepted: 20 January 2025

DOI: 10.1002/ar.25638

RESEARCH ARTICLE

The Anatomical Record WILEY

Variability of jaw muscles in Tunisian street dogs and adaptation to skull shape

Colline Brassard[1,2] | **Lobna Wertani**[3] | **Anthony Herrel**[1,4,5,6] | **Hassen Jerbi**[3,7]

[1]UMR 7179 MECADEV: Mécanismes adaptatifs et évolution, MNHN-CNRS, Paris, France

[2]VetAgro Sup, Campus Vétérinaire de Lyon, Marcy l'Etoile, France

[3]Service of Anatomy, National School of Veterinary Medicine of Sidi Thabet, Tunisia

[4]Department of Biology, Evolutionary Morphology of Vertebrates, Ghent University, Ghent, Belgium

[5]Department of Biology, University of Antwerp, Wilrijk, Belgium

[6]Naturhistorisches Museum Bern, Bern, Switzerland

[7]University of Manuba, Tunis, Tunisia

Correspondence
Colline Brassard, VetAgro Sup, Campus Vétérinaire de Lyon, 1 avenue Bourgelat 69260 Marcy l'Etoile, France.
Email: colline.brassard@vetagro-sup.fr

Funding information
Fondation Fyssen

Abstract

The impact of artificial selection on the masticatory apparatus of dogs has been poorly studied, and comparative data with dogs subjected to more natural constraints are lacking. This study explores the jaw musculature of Tunisian street dogs, which are largely free from the influence of breed-specific selection. The masticatory muscles (digastric, masseter, temporalis, and pterygoid) of 27 adult dogs were dissected and muscle mass and physiological cross-sectional area (PCSA) were quantified, providing a baseline for comparisons between dogs from more natural versus more controlled environments. Our findings reveal that the morphology of the jaw adductor muscles is remarkably conserved among dogs, despite significant variation in skull shape. Additionally, all masticatory muscles scale isometrically with body mass. Notably, females exhibit functional adaptations that optimize muscle strength, particularly in the temporalis muscle, despite showing smaller overall muscle volumes compared to males. This could be linked to differences in predation, competition for food, or factors related to sexual behavior. Preliminary evidence suggests that captivity may limit the development of muscle mass and PCSA in the temporalis muscle, likely due to changes in lifestyle and diet. Significant relationships were also observed between skull shape and muscle data, particularly in the mandible, indicating that skull variability reflects jaw adductor muscle anatomy to some degree. This study enhances our understanding of jaw muscle morphology and function in feral dog populations and offers insights into the adaptation of the masticatory apparatus in dogs.

KEYWORDS

artificial selection, dog, jaw, mandible, skull

1 | INTRODUCTION

1.1 | Overview of the masticatory apparatus in dogs

Studying masticatory muscles in carnivorans and canids provides valuable insights into their evolutionary adaptations for hunting and processing prey as the muscles are directly related to diet, prey capture, and predatory behavior (Anderson et al., 2008; Christiansen & Wroe, 2007; Wroe & Milne, 2007). The study of the jaw muscles may thus provide insights into adaptive variation in relation to variation in ecology. In domestic dogs, these muscles likely have adapted to changes in diet resulting from domestication, which often includes a broader variety of foods. Dietary variation—ranging from meat-heavy diets in wild canids to more diverse meals in pets—affects jaw function and muscle development. Comparative studies across different wild carnivoran or canid species, or even across dog breeds, reveal significant differences in muscle structure and function (e.g., Brassard, Merlin, Guintard, Monchâtre-Leroy, Barrat, Bausmayer, et al., 2020a; Brassard, Merlin, Monchâtre-Leroy, et al., 2020; Hartstone-Rose et al., 2022; Ito & Endo, 2016; Penrose et al., 2020). These species-specific adaptations shed light on the diverse feeding behaviors and physical traits observed among different dog breeds. However, studies comparing wild and domestic species are lacking.

The performance of the jaw apparatus can be apprehended by measuring or estimating bite force, which is determined by the architectural properties of muscles and their moment arms (Anderson et al., 2008; Kim et al., 2018). These, in turn, depend on the morphology and spatial configuration of the specific attachment sites on the cranium and mandible for the muscles responsible for the mandible elevation (called jaw adductors: masseter, temporal and pterygoid muscles; Hartstone-Rose et al., 2012). Jaw opening is primarily a passive phenomenon resulting from the relaxation of the jaw adductors, but it also involves the contraction of the digastric muscle.

Functional relationships between the muscular and bony components of the jaw apparatus in carnivorans have been the subject of many studies (Hartstone-Rose et al., 2012, 2022; Ito & Endo, 2016, 2019; Ito et al., 2024; Penrose et al., 2016, 2020). However, most of these studies have focused on broad taxonomic comparisons (especially Carnivora, Canidae, or Felidae) but with a reduced sample size for each species. Only a few studies have examined the variability within a single species (e.g., Brassard et al., 2021; Brassard, Forbes-Harper, et al., 2022). Among the latter, only a few have focused on dogs *Canis lupus familiaris* (e.g., Brassard, Merlin, Guintard, Monchâtre-Leroy, Barrat, Bausmayer, et al., 2020a; Brassard, Merlin, Guintard, Monchâtre-Leroy, Barrat, Callou, et al., 2020b; Brassard, Merlin, Monchâtre-Leroy, et al., 2020), despite the tremendous diversity of breeds offering a unique opportunity to explore the consequences of morphological diversity on the functional relationships of the masticatory apparatus.

Previous studies have demonstrated strong relationships between muscle strength and cranial and mandibular shape, likely driven by genetic constraints. These relationships are promising for making functional inferences in the archaeological record and deciphering the impact of human selection over time. However, when considering ancient times (particularly between dog domestication 15,000 years ago and the Bronze Age), modern breeds are not good models because part of the past diversity has since disappeared (Brassard, Bălăşescu, et al., 2022) and ancient dogs were unlikely to have been as extremely artificially selected as modern breeds are (since the late 19th century). Unfortunately, previous studies lack data on dogs that are not artificially selected for specific tasks or aesthetic reasons and are more subject to natural constraints.

1.2 | Street dogs as a model for studying the impact of natural constraints on the masticatory apparatus

Street dogs (i.e., free-ranging, unowned dogs that live and roam in urban or rural areas without direct human supervision or care) are excellent subjects for addressing this gap. Unlike 'companion dogs,' which are owned and cared for by individuals or families and typically live within households, street dogs rely on scavenging or community feeding for subsistence. Our focus on street dogs is particularly relevant because their behaviors—such as hunting, diet, and movement patterns—can differ significantly from those of companion dogs, providing a unique opportunity to explore the impact of natural selection as opposed to strong human control. Interestingly, stray/mongrel dogs from all geographic locations (Asia, Africa, etc.) display morphological convergence to an average-sized dog, similar to a golden retriever, most often with a beige coat. This convergence likely arises from adaptation to similar niches by different lineages.

In the present study, we focus on the jaw apparatus of street dogs from Tunisia. Street dogs in Tunisia exhibit characteristics similar to the Atlas Mountain Dog, or Aidi, a rustic breed native to the Atlas Mountains of North Africa (United Kennel Club, 2022). The Aidi, predominantly found in Morocco, has traditionally provided protection against wildcats, predators, and strangers (Grandjean, 2010). The breed has also been utilized by Berber tribes as a protector for desert nomad camps. The Aidi is present in Algeria, Tunisia, and Libya, and is noted for its lean, muscular body,

coarse and thick weather-resistant coat, and strong jaws. There are two hypotheses regarding the origins of the Aidi: it may have been bred by the Phoenicians between 1550 and 300 B.C., or it may have developed in the Atlas Mountains and later spread with nomadic people to the Pyrenees Mountains, potentially influencing the modern Pyrenean Mountain Dog. The Aidi stands 52–62 cm in height, weights around 25 kg, and has a variety of coat colors, including white, black, pale red, and tawny (Figure 1b). A club has recently been formed in Morocco to preserve the breed's purity due to its significant contributions as a protector, hunter, police dog, and companion. The street dogs in Tunisia, showing resemblance to the Aidi, provide a unique opportunity to study the functional relationships within the jaw apparatus in a strongly human-modified context but without strong artificial selection.

1.3 | Current methods for quantifying jaw function

Two main methods allow to measure or estimate muscle strength or bite force: in vivo measurements of bite force using transducers, or the combination of the physiological cross-sectional area (PCSA, a proxy of muscle force) of muscles with dimensions on the skull that approximate moment arms of the muscles and of the bite point (Brassard, Merlin, Guintard, Monchâtre-Leroy, Barrat, Bausmayer, et al., 2020a; Hartstone-Rose et al., 2012). Additionally, finite element analyses (Bourke et al., 2008; Ruiz et al., 2023) allows to explore how stresses and strains due to biting are distributed across the skull. Estimations of the PCSA can be made from gross dissection, or using the dry skull method which consists in applying equations based on skull measurements reflecting the geometric surface of insertion of the jaw adductors (e.g., Christiansen & Adolfssen, 2005; Christiansen & Wroe, 2007; Damasceno et al., 2013; Ellis et al., 2008, 2009; Forbes-Harper et al., 2017; Thomason, 1991; Wroe et al., 2005; Wroe & Milne, 2007). Dissection allows to quantify muscle architecture more precisely (mass, fiber length, and pennation angle) and thus to estimate PCSA much more accurately than the dry skull method (Ito et al., 2024; Law & Mehta, 2019). Indeed, the dry-skull method may overestimates PCSA of the masseter and underestimates PCSA of the temporalis (Law & Mehta, 2019).

FIGURE 1 Provenance and appearance of the specimens considered in the study. (a) Map indicating the area of provenance (in blue) of the specimens, in a perimeter surrounding the Veterinary school of Sidi Thabet. (b) A typical Aidi dog (© https://www.roysfarm.com/aidi-dog/). (c) A free-roaming Tunisian street dogs in Sidi-Thabet, typical of those we dissected (© Colline Brassard).

However, dissection data providing insights into the intraspecific variability are scarce for dogs, most of the studies focusing on small datasets. Moreover, no data are available for street dogs to date.

In the present study, we describe the architectural properties (mass and PCSA as a proxy for muscle force) of the masticatory muscles (digastric, temporal, masseter, and pterygoid muscles) in adult Tunisian street dogs from a limited area. These dogs exhibit either a free-roaming lifestyle or a human-controlled lifestyle (and diet) with restricted mobility. We [1] quantify the variability in muscle mass and PCSA in the whole sample, as well as for each group and sex, [2] explore scaling with a number of size proxies (body mass, skull length, and mandible length), [3] test for sexual dimorphism in muscle data and [4] investigate the integration between skull shape or mandible shape and muscle mass and PCSA to determine whether functional inferences can be made from bone shape. We expect limited variation in the architectural data and significant relationships between bone shape and muscle architecture, with stronger relationships for the mandible, as it is more focused on masticatory function compared to the skull, which also protects and houses the brain and major sensory systems.

2 | MATERIALS AND METHODS

2.1 | Sample

We dissected the masticatory muscles of 27 adult dogs (all with fully erupted permanent teeth). All the dogs exhibited the typical morphology of Tunisian free-roaming street dogs, with traits resembling those of the Aidi (Figure 1b,c). The average body mass was 19.0 ± 4.1 kg, and the average height at the withers was 52.3 ± 5.0 cm, with females being smaller than males (Table 1).

The dogs were divided into two groups based on their lifestyle. The stray group consisted of freshly deceased dogs from roadkill, collected by the anatomy department of the veterinary school of Sidi Thabet, located 30 km northwest of Tunis (Figure 1a). The captive group included dogs originally from the same population (taken from the street at 8–12 months old) but kept in captivity for 2 years, after which they were euthanized as part of a previous experiment approved by an Ethics Committee (approval number: CEEA-ENMV 12/20). These dogs had restricted mobility, housed in two 30 m^2 yards during the day and in cages at night, and were fed on a controlled diet (dog kibble) for 2 years.

Our primary aim was to quantify the jaw muscles in street dogs with limited human control, making the "Stray" sample the focus of the analyses in this study. Whilst the small size of the captive group limits robust statistical exploration of the impact of captivity on muscle architecture, preliminary analyses of this group are included to provide a baseline for future research. Additionally, we present results from analyses conducted on the entire sample to capture a broader range of morphological diversity, which is particularly useful for examining covariation between muscle and shape data.

The specimens were maintained in a frozen state at −19°C before dissection.

2.2 | Dissections

During dissection, we assessed muscle integrity and excluded any samples exhibiting significant decomposition, such as abnormal texture, odor, or loss of structural definition. This careful selection ensured that the analyzed muscle characteristics were both representative and reliable.

The masticatory muscles are represented by the digastric, masseter, temporal, and pterygoid muscles. The digastric muscle is the only muscle responsible for opening the mouth. Data of the two bellies were recorded separately. The other muscle complexes are jaw elevators (or jaw adductors) or muscles that function to stabilize the jaw joint. The different bellies of the jaw adductors were macroscopically identified following the descriptions in Penrose et al. (2016) and Brassard, Merlin, Monchâtre-Leroy, et al. (2020), respecting the nomenclature of

TABLE 1 Details of specimens, with sample size, mean and standard deviation of the bodymass and withers heights for all groups considered in this study.

	Females			Males		
	n	Body mass (kg)	Wither height (cm)	*n*	Body mass (kg)	Wither height (cm)
Captive	4	17.4 ± 2.9	49.6 ± 5.3	3	22.9 ± 4.1	56.7 ± 3.8
Stray	9	16.1 ± 3.2	50.3 ± 4.9	11	20.8 ± 3.4	53.6 ± 4.7
All by sex	13	16.5 ± 3.1	50.1 ± 4.8	14	21.3 ± 3.5	54.3 ± 4.6
All	$N = 27$	Body mass = 19.0 ± 4.1 kg		Wither height = 52.3 ± 5.0 cm		

previous authors (Druzinsky et al., 2011; Ström et al., 1988; Tomo et al., 1993; Turnbull, 1970).

We thus considered during dissections the digastricus pars rostralis, digastricus pars caudalis, masseter pars superficialis, masseter pars profunda, masseter pars zygomaticomandibularis anterior and posterior, temporalis pars suprazygomatica, temporalis pars superficialis, temporalis pars profunda, pterygoideus medialis and pterygoideus lateralis (Figure 2).

After identification, all muscle divisions were isolated and a series of measurements were performed to quantify jaw muscle architecture. We measured muscle mass using a digital scale. We then measured fiber length and pennation angle (Figure 2) after sectioning the muscles along their line of action. Several measurements were taken at different locations along the muscle, and we used the mean for our subsequent calculations. We used these data to calculate the PCSA, which represents a proxy of the intrinsic strength of the muscles (Haxton, 1944), and using a muscle density of 1.06 g/cm^3 (Méndez & Keys, 1960). We used the following formula, which, as well as muscle mass and fascicle length, also considers the effect of the pennation angle of the fascicles, providing a more accurate approximation of the maximal strength produced by each muscle.

$$\mathrm{PCSA} = \frac{\mathrm{mass(g)} \times \cos(\mathrm{angle\ of\ pennation\ (rad)})}{1.06(\mathrm{g/cm^3}) \times \mathrm{fiber\ length\ (cm)}}$$

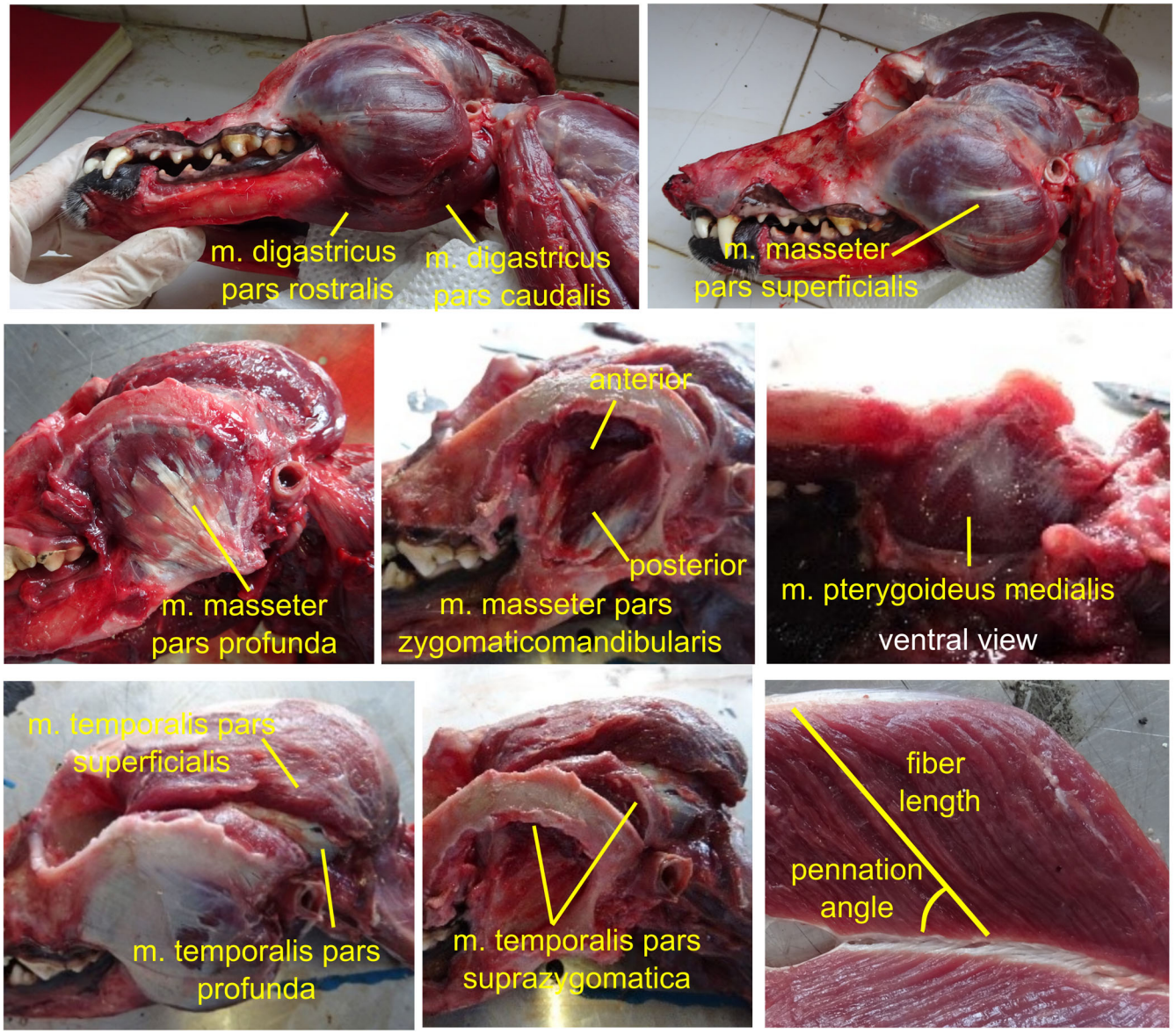

FIGURE 2 Photos of the different muscle bundles dissected in this study. Only the lateral pterygoid is not shown. The last picture shows the aspect of the deep temporal muscle (m. *temporalis pars profunda*) after sectioning the muscle along its line of action.

2.3 | Shape analyses

After dissection, the skulls were cleaned by boiling them for several hours to ensure the removal of any remaining tissue.

Three-dimensional numerical models of the crania and right dentaries were obtained using photogrammetry. For each bone, 100 photographs were taken from different angles by rotating the bone on a turning table, using a Nikon D5500 Camera (24.2 effective megapixels) equipped with a 40–120 mm lens. The photos were then processed into 3D numeric models using 'Agisoft Metashape' (version 2.1.1, ©2014 Agisoft LLC, St Petersburg, Russia). A complete protocol is provided in the supplementary material of Brassard et al. (2023). The external surfaces of the numeric models were repaired (filling of small holes), cleaned, simplified using © 'Geomagic Wrap' 2013.0.1.1206 and 'MeshLab' v 2020.03 (Cignoni et al., 2008). All the 3D models are available on Sketchfab.

Three-dimensional landmarks were placed on the 3D models using the 'Landmark' software, version 3.0.0.6 (©IDAV, 2002–2005; Wiley et al., 2005). For the cranium, 42 landmarks were placed on one side (Figure 3, a detailed description of landmarks is provided in Appendix S1). A mirror function (function 'mirrorfill' from the package 'paleomorph') was then applied to obtain the symmetrical landmarks relative to the sagittal for further visualization. However, statistical analyses were performed on the 42 landmarks only. The protocol for the mandible comprises 25 landmarks (Figure 3, a detailed description of the landmarks is provided in Appendix S1).

All statistical analyses were run in 'R' version 4.0.0 (2020-04-24) (R Core Team, 2021).

To break down the cranium or mandible form into centroid size (a proxy of the overall size of the object) and shape (which represents the proportions based on the differences between the different landmarks), we performed a Generalized Procrustes analyses (GPA) (Goodall, 1991) using the function 'procSym' (Dryden & Mardia, 2016; Gunz et al., 2005; Klingenberg et al., 2002) from the package 'Morpho.' Separate GPAs were performed for all sets of data. An intact (not fragmented) cranium and mandible were warped to the consensus of the GPA using thin-plate spline deformation for all further visualizations (Klingenberg, 2013).

2.4 | Statistical analyses

To describe the variability in muscle architecture (mass and PCSA) of the masticatory muscles (digastric, temporal, masseter, and pterygoid muscles) we used simple

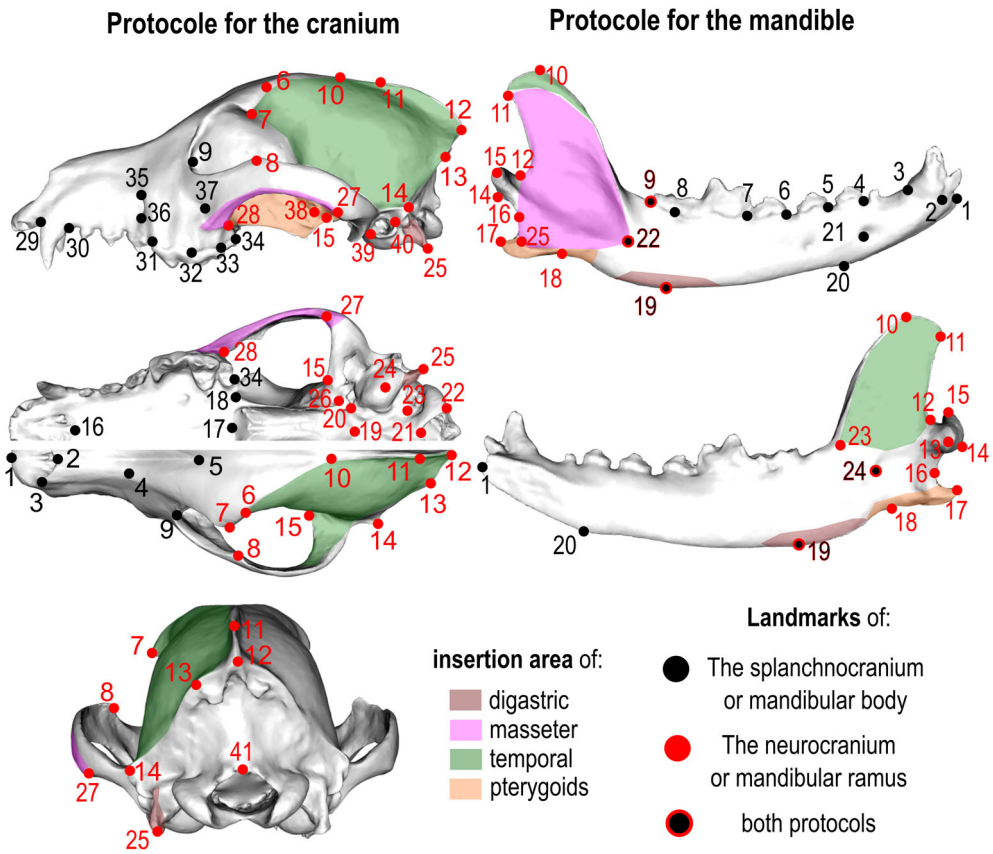

FIGURE 3 Landmarking protocols for the cranium and mandible. The landmarks used to distinguish the rostral and caudal parts of the cranium and mandible are indicated in different colors. Detailed descriptions are provided in Appendix S1. The area of origin and insertion of the masticatory muscles are indicated in colors.

descriptive statistics (mean, standard deviation, SD), by considering the sample as a whole, and after splitting the data by sex and by living conditions. To limit noise in the data and make statistical analyses more robust, we summed the mass or PCSA of each muscle bundle to consider the digastric as the sum of its two bellies, the masseter complex (containing the masseter pars superficialis, pars profunda, pars zygomaticomandibularis anterior and posterior), the temporal complex (grouping the m. temporalis pars suprazygomatica, superficialis and profunda) and the pterygoids (grouping m. pterygoideus medialis and lateralis). We explored variability in raw data in each muscle group, and then the variability in the proportion of the jaw adductors only (i.e., masseter, temporal, and pterygoid groups). The sample size in the captive group was too small to provide any statistical comparisons with the free-roaming group but raw data and visualizations of variation are provided for information and discussion.

Second, we explored scaling in muscle data ($mass^{1/3}$ and $PCSA^{1/2}$) with different size proxies (body mass, skull or length, skull or mandible centroid size), using ANOVAs (function 'aov') and linear models (function 'lm'). We did not use RMA analyses because "the concerns that arise from measurement error for OLS regression are small and straightforward to deal with, whereas RMA has several key properties that make it unfit for use in the field of allometry" (Kilmer & Rodríguez, 2017). Cranial length corresponds to the Euclidean distance between landmarks 1 and 21 and mandible length to the distance between landmarks 1 and 12. Evaluations of isometry were made based on the slope 95% confidence intervals and the parameter offset in the 'lm' function. For these analyses, we considered the whole sample. All data were $\log_{10}$-transformed. We expect to find isometric relationships, in according with previous studies based on carnivorans ("all jaw adductor muscles scale isometrically against body mass, regardless of phylogeny or trophic group"; Penrose et al., 2016).

Third, we explored the differences in musculature between sexes in the free-roaming group. We first compared the bodymasses and the raw masses and PCSAs of the jaw muscles between sexes using one-sided Wilcoxon Rank-Sum tests. We then explored differences in scaled muscle data between sexes in free-roaming dogs using one-sided Wilcoxon Rank-Sum test. To do so, and to visualize the variability within groups using boxplots, we considered the following ratios:

$$\text{scaled mass} = \frac{\text{muscle mass}^{1/3}}{\text{bodymass}^{1/3}} \text{ and scaled PCSA} = \frac{\text{muscle PCSA}^{1/2}}{\text{bodymass}^{1/3}}$$

We also tested for differences in proportions between sexes using one-sided Wilcoxon Rank-Sum test. For all these tests, we considered p values under 0.10 (and not 0.05) because of the small sample size in each sex.

Fourth, we explored the relationship between muscle data (relative mass and PCSA) and skull shape. To determine the amount of variation in shape explained by variation in each muscle data, we performed a series of Procrustes ANOVAs/regressions with permutation procedures on the shape coordinates (of the cranium or mandible), residual muscle mass and PCSA data using the function 'procD.lm' with 1000 iterations (Adams & Collyer, 2016, 2017; Anderson, 2001; Anderson & Braak, 2003; Collyer et al., 2015; Goodall, 1991). Residual muscle masses and PCSAs were the residuals of the regression of the $\log_{10}(mass^{1/3})$ or $\log_{10}(PCSA^{1/2})$ to the $\log_{10}(bodymass^{1/3})$. We performed several simple regressions on the coordinates from the GPA for the complete cranium or mandible, and the shape of the rostral or caudal parts of the cranium and mandible. Second, to explore the covariation patterns between bone shape and muscle data, we performed two-block partial least squares analyses (2B-PLS) with the function 'pls2B' (Rohlf & Corti, 2000). p-values (attesting to the significance of the covariations) were computed from 1000 permuted blocks. We performed analyses on the complete shape of the cranium and mandible and after that by separating the rostral and caudal parts of the cranium and mandible (Figure 3). We predict that the caudal parts (neurocranium and coronoid process of the mandible) show better covariations than the rostral part as they consist of the area of insertion of the masticatory muscles. In the analyses, we considered the mass and PCSA scaled to the body mass, skull length or mandible length using the residuals of linear regressions.

3 | RESULTS

3.1 | Variability in architectural properties of the masticatory muscles

The mean values of the masses (g) and PCSAs (cm^2) of all masticatory muscles and the proportions of the different adductors are reported in Table 2. The temporalis group contributed around 64.1 ± 2.0% to the total muscle mass of the adductors, the masseter group contributed around 26.2 ± 1.7% and the pterygoids contributed around 9.8 ± 0.9%. With regard to the PCSAs, the temporalis group contributed around 50.4 ± 4.8%, the masseter group contributed around 35.6 ± 4.2%, and the pterygoids contributed around 13.9 ± 2.6% of the total PCSA of the adductor muscles. The lateral pterygoid represents only 4.8 ± 1.7% of the mass of the medial pterygoid or 0.47 ± 0.18% of the total mass of the jaw adductors.

TABLE 2 Variability in raw muscle mass (g), raw PCSA ($N.cm^{-2}$) of all masticatory muscles, and proportions of adductor muscles (indicated in parentheses).

	Bodymass (kg)	Digastric mass	Temporalis mass	Masseter mass	Pterygoid mass	Total jaw adductor mass	Digastric PCSA	Temporalis PCSA	Masseter PCSA	Pterygoid PCSA	Total jaw adductor PCSA
All	19.0 ± 4.1	16.2 ± 4.1	94.8 ± 25.6 (64.1 ± 2.0%)	38.6 ± 1.1 (26.2 ± 1.7%)	14.3 ± 3.3 (9.8 ± 0.9%)	147.7 ± 39.3	1.9 ± 0.3	23.9 ± 6.1 (50.4 ± 4.8%)	16.8 ± 4.2 (35.6 ± 4.2%)	6.6 ± 2.1 (13.9 ± 2.6%)	47.3 ± 10.9
Captive females	17.4 ± 2.9	14.9 ± 2.4	88.2 ± 21.0 (64.1 ± 0.4%)	36.4 ± 8.8 (26.4 ± 0.5%)	13.1 ± 2.7 (9.6 ± 1.0%)	138 ± 32.0	1.9 ± 0.2	21.7 ± 4.0 (49.6 ± 2.5%)	16.8 ± 5.7 (37.6 ± 4.4%)	5.5 ± 0.7 (12.8 ± 2.2)	44.0 ± 10.0
Stray Females	16.1 ± 3.3	12.83 ± 2.3	75.9 ± 16.3 (64.3 ± 1.1%)	29.8 ± 5.4 (25.4 ± 1.1%)	11.9 ± 1.9 (10.3 ± 1.1%)	117.6 ± 23.1	1.6 ± 0.3	23.8 ± 6.1 (53.2 ± 5.5%)	14.7 ± 2.9 (33.2 ± 3.1%)	6.0 ± 1.8 (13.6 ± 3.0)	44.5 ± 9.2
Captive males	22.9 ± 4.1	19.0 ± 2.4	120.2 ± 29.5 (63.7±	50.2 ± 4.4 (27.2 ± 2.7%)	17.1 ± 2.9 (9.2 ± 0.4%)	188 ± 36.6	2.1 ± 0.2	25.6 ± 6.1 (47.7 ± 2.2%)	18.9 ± 2.6 (35.9 ± 6.0%)	8.9 ± 3.5 (16.4 ± 3.8)	53.4 ± 11.0
Stray Males	20.8 ± 3.4	18.7 ± 4.2	105.6 ± 22.7 (64.1±)	43.6 ± 11.5 (26.3 ± 1.9%)	16 ± 3.3 (9.7 ± 0.7%)	165 ± 36.8	2.0 ± 0.4	24.3 ± 7.3 (49.2 ± 4.7%)	18.0 ± 4.6 (36.9 ± 3.9%)	6.8 ± 2.1 (13.9 ± 1.8)	49.1 ± 12.8

3.2 | Scaling of muscle data

The scaling relationships between muscle data and different proxies of size are reported in Table 3.

We find that muscle traits (mass and PCSA) of all masticatory muscles (as well as the adductors grouped together) scale isometrically with size, for almost all proxies including body mass. However, we find evidence of negative allometry between the mass or PCSA of the digastric or the mass of the pterygoid and the centroid size of the neurocranium and mandibular ramus (Table 3), which is probably related to its limited area of insertion on these parts of the bones (see Figure 2).

All size proxies explain more of the variability in muscle mass than in muscle PCSA. The (total and individual) masses of the adductor muscles are better predicted by size (whatever the proxy) than the mass of the digastric. The best predictor of the mass of the digastric is the body mass (which explains 64% of the variability). The best predictors of the adductor masses are the body mass (explains 75% of the variability), the centroid size of the neurocranium (73%), followed by the centroid size of the mandibular ramus, to a lesser extent (65%). When considering the PCSA, the best predictor among body mass or centroid size depends on the muscle being analyzed. The PCSA of the masseter is best explained by size, irrespective of the proxy used. The best predictors of the PCSA of the masseter are the body mass (38%), the centroid size of the neurocranium (45%), followed by the centroid size of the mandibular ramus (34%). We notice that the centroid size of the complete cranium or complete mandible are as efficient for predicting muscle masses or PCSAs (same coefficients of determination).

Between the different parts of the cranium, the centroid size of the neurocranium is clearly a better predictor of muscle mass and PCSA than the size of the complete bone or of the rostral part only. However, for the mandible, the differences when considering the size of the total bone or only that of the rostral or posterior parts are less clear. The centroid size of the neurocranium explains more of the variability in adductor mass and masseter PCSA than the centroid size of the mandibular ramus.

3.3 | Differences between sexes

Males have more important masses than females of the digastric and all jaw adductors ($p < 0.002$ for all muscles), which is related to significant differences in the body mass (Table 2, $p = 0.003$). The difference in raw values is significant for the PCSA for the digastric ($p = 0.005$) and the masseter ($p_{masseter} = 0.07$), but not for the other jaw adductors (Figure 4, $p_{temporal} = 0.4$; $p_{pterygoids} = 0.2$; $p_{all\ adductors} = 0.2$).

TABLE 3 Results of the linear regressions between muscle data (mass$^{1/3}$ and PCSA$^{1/2}$) and different proxies of size (bodymass$^{1/3}$, length or centroid size of the cranium, neurocranium, rostral part of the cranium and mandible).

Muscle data	Size proxy	Muscles	*p*	R^2	Slope (and 95% CI)	*p*-value to test slope = 1	Conclusion
Mass$^{1/3}$	Bodymass$^{1/3}$	Digastric	***	0.64	0.9 (0.6–1.2)	0.7	Isometry
		All adductors	***	0.75	1.1 (0.8–1.3)	0.5	Isometry
		Masseter	***	0.78	1.2 (0.9–1.4)	0.2	Isometry
		Temporal	***	0.69	1.1 (0.8–1.4)	0.6	Isometry
		Pterygoids	***	0.81	1.0 (0.8–1.2)	0.8	Isometry
	Cranial centroid size	Digastric	***	0.45	0.8 (0.5–1.2)	0.3	Isometry
		All adductors	***	0.61	1.0 (0.7–1.3)	0.9	Isometry
		Masseter	***	0.64	1.1 (0.7–1.4)	0.7	Isometry
		Temporal	***	0.56	1.0 (0.6–1.3)	0.8	Isometry
		Pterygoids	***	0.73	0.9 (0.7–1.2)	0.5	Isometry
	Splanchnocranium centroid size	Digastric	***	0.44	0.83 (0.46–1.2)	0.9	Isometry
		All adductors	***	0.60	1.0 (0.7–1.3)	0.9	Isometry
		Masseter	***	0.63	1.1 (0.76–1.4)	0.5	Isometry
		Temporal	***	0.54	0.99 (0.6–1.3)	0.9	Isometry
		Pterygoids	***	0.71	0.94 (0.7–1.2)	0.7	Isometry
	Neurocranium centroid size	Digastric	***	0.54	0.88 (0.6–1.2)	0.4	Isometry
		All adductors	***	0.73	1.1 (0.8–1.3)	0.8	Isometry
		Masseter	***	0.73	1.1 (0.9–1.4)	0.4	Isometry
		Temporal	***	0.68	1.1 (0.77–1.4)	0.9	Isometry
		Pterygoids	***	0.77	0.9 (0.7–1.2)	0.8	Isometry
	Cranial length	Digastric	***	0.43	0.8 (0.4–1.2)	0.4	Isometry
		All adductors	***	0.57	1.0 (0.6–1.3)	0.8	Isometry
		Masseter	***	0.62	1.1 (0.7–1.4)	0.4	Isometry
		Temporal	***	0.50	0.9 (0.6–1.3)	0.9	Isometry
		Pterygoids	***	0.70	0.9 (0.7–1.1)	0.4	Isometry
	Mandible centroid size	Digastric	***	0.45	0.8 (0.4–1.1)	0.2	Isometry
		All adductors	***	0.61	0.96 (0.7–1.3)	0.8	Isometry
		Masseter	***	0.65	1.0 (0.7–1.4)	0.8	Isometry
		Temporal	***	0.55	0.9 (0.6–1.3)	0.7	Isometry
		Pterygoids	***	0.74	0.9 (0.7–1.1)	0.4	Isometry
	Mandibular body centroid size	Digastric	***	0.44	0.8 (0.5–1.2)	0.3	Isometry
		All adductors	***	0.60	0.99 (0.7–1.3)	0.9	Isometry
		Masseter	***	0.61	1.1 (0.7–1.4)	0.7	Isometry
		Temporal	***	0.54	1.0 (0.6–1.3)	0.8	Isometry
		Pterygoids	***	0.74	0.9 (0.7–1.2)	0.6	Isometry
	Mandibular ramus centroid size	Digastric	***	0.49	0.7 (0.4–0.9)	0.041	Negative allometry
		All adductors	***	0.65	0.8 (0.6–1.1)	0.2	Isometry
		Masseter	***	0.72	0.9 (0.7–1.1)	0.4	Isometry
		Temporal	***	0.58	0.8 (0.5–1.1)	0.2	Isometry
		Pterygoids	***	0.71	0.7 (0.5–0.9)	0.034	Negative allometry

(Continues)

TABLE 3 (Continued)

Muscle data	Size proxy	Muscles	p	R^2	Slope (and 95% CI)	p-value to test slope = 1	Conclusion
	Mandible length	Digastric	***	0.48	0.8 (0.4–1.1)	0.14	Isometry
		All adductors	***	0.61	0.9 (0.6–1.2)	0.5	Isometry
		Masseter	***	0.65	0.99 (0.7–1.3)	0.9	Isometry
		Temporal	***	0.54	0.88 (0.5–1.2)	0.9	Isometry
		Pterygoids	***	0.73	0.85 (0.6–1.1)	0.14	Isometry
PCSA$^{1/2}$	bodymass$^{1/3}$	Digastric	0.002	0.28	0.74 (0.29–1.2)	0.3	Isometry
		All adductors	0.002	0.30	0.93 (0.37–1.5)	0.8	Isometry
		Masseter	***	0.38	1.1 (0.54–1.6)	0.7	Isometry
		Temporal	0.03	0.15	0.77 (0.10–1.4)	0.5	Isometry
		Pterygoids	0.011	0.20	1.0 (0.3–1.8)	0.9	Isometry
	Cranial centroid size	Digastric	0.03	0.14	0.55 (0.05–1.1)	0.08	Isometry
		All adductors	0.008	0.21	0.82 (0.22–1.4)	0.5	Isometry
		Masseter	***	0.32	1.0 (0.4–1.6)	1.0	Isometry
		Temporal	0.07	0.10	0.6 (−0.13–1.3)	0.2	Isometry
		Pterygoids	0.002	0.31	1.3 (0.5–2.0)	0.5	Isometry
	Splanchnocranium centroid size	Digastric	0.04	0.12	0.5 (0.02–1.1)	0.2	Isometry
		All adductors	0.009	0.21	0.83 (0.22–1.4)	0.5	Isometry
		Masseter	0.004	0.26	0.96 (0.3–1.6)	0.9	Isometry
		Temporal	0.08	0.08	0.6 (−0.09–1.4)	0.2	Isometry
		Pterygoids	***	0.31	1.3 (0.6–2.1)	0.7	Isometry
	Neurocranium centroid size	Digastric	0.01	0.18	0.6 (0.1–1.1)	0.2	Isometry
		All adductors	***	0.32	0.97 (0.4–1.5)	0.5	Isometry
		Masseter	***	0.45	1.2 (0.7–1.7)	0.8	Isometry
		Temporal	0.04	0.13	0.74 (0.06–1.4)	0.2	Isometry
		Pterygoids	***	0.34	1.3 (0.6–2.0)	0.6	Isometry
	Cranial length	Digastric	0.02	0.16	0.6 (0.09–1.1)	1.0	Isometry
		All adductors	0.017	0.17	0.75 (0.14–1.4)	0.4	Isometry
		Masseter	0.002	0.29	1.0 (0.4–1.6)	0.9	Isometry
		Temporal	0.15	-	-	-	
		Pterygoids	0.007	0.23	1.1 (0.3–1.9)	0.8	Isometry
	Mandible centroid size	Digastric	0.03	0.14	0.54 (0.05–1.0)	0.06	
		All adductors	0.013	0.19	0.75 (0.17–1.3)	0.4	Isometry
		Masseter	0.0019	0.30	0.96 (0.4–1.5)	0.8	Isometry
		Temporal	0.12	-	-	-	
		Pterygoids	0.0043	0.26	1.1 (0.4–1.9)	0.18	Isometry
	Mandibular body centroid size	Digastric	0.034	0.14	0.6 (0.05–1.1)	0.11	Isometry
		All adductors	0.016	0.18	0.8 (0.16–1.4)	0.4	Isometry
		Masseter	0.0028	0.28	0.97 (0.37–1.6)	0.9	Isometry
		Temporal	0.13	-	-	-	
		Pterygoids	0.0042	0.26	1.2 (0.41–2.0)	0.9	Isometry
		Digastric	0.041	0.12	0.42 (0.02–0.83)	0.02	Negative allometry

TABLE 3 (Continued)

Muscle data	Size proxy	Muscles	p	R^2	Slope (and 95% CI)	p-value to test slope = 1	Conclusion
	Mandibular ramus centroid size	All adductors	0.007	0.22	0.7 (0.2–1.1)	0.10	Isometry
		Masseter	***	0.34	0.8 (0.4–1.3)	0.4	Isometry
		Temporal	0.07	0.09	0.5 (−0.04–1.1)	0.05	
		Pterygoids	0.013	0.19	0.8 (0.2–1.5)	0.7	Isometry
	Mandible length	Digastric	0.028	0.15	0.5 (0.05–0.98)	0.04	
		All adductors	0.022	0.16	0.7 (0.10–1.2)	0.2	Isometry
		Masseter	0.0034	0.27	0.86 (0.3–1.4)	0.6	Isometry
		Temporal	0.15	-	-	-	
		Pterygoids	0.014	0.19	0.9 (0.2–1.7)	0.9	Isometry

Note: ***p-value <0.001. CI, 95% confidence interval.

Relative masses (g) and relative PCSAs (cm^2) of the individual jaw muscles are presented in Figure 4. One-sided Wilcoxon-tests revealed that females tend to have lower relative muscle masses for the digastric ($p = 0.06$), masseter ($p = 0.06$) and temporal ($p = 0.11$) muscles and consequently for the total mass of the adductor muscles ($p = 0.10$). There is no significant difference between sexes for the pterygoids for the mass ($p = 0.25$). As for PCSAs, females tend to have greater relative PCSAs of temporal muscle ($p = 0.10$) but there is no significant difference for the other muscles ($p > 0.3$). Qualitatively, the differences in relative masses between females and males tend to be the same in the captive dogs (Figure 4). However, for both sexes, the relative values of the temporalis seem limited to low values in the captive dogs compared to the free-roaming dogs (Figure 4) but this remains preliminary given the small sample size.

The proportions of the different adductor muscles show significant differences between sexes in the free-roaming dogs. The PCSA of the masseter is significantly more important in males ($p = 0.006$) whilst the PCSA of the temporal is greater in females ($p = 0.033$). The difference is not significant for masses (masseter: $p = 0.09$; temporal: $p = 0.4$). There is no difference for the pterygoid (mass: 0.2; PCSA: $p = 0.6$). Qualitatively, the differences in mass proportions between females and males tend to be the same in the captive dogs (Figure 4, Table 2), but there seems to be different patterns with regard to the PCSA.

3.4 | Correlations and covariations between muscle data and shape data

The Procrustes ANOVAs (Table 4) show no correlation between digastric mass or PCSA and bone shape. The total mass of the jaw adductors is correlated with cranial shape but not mandible shape. The total mass explains almost the same amount of variation in the shape of both bones. However, we obtain better correlations when considering the shape of the posterior part of the cranium. The analyses performed on separate muscles show that the mass of the temporal and pterygoid muscles correlates with the shape of the neurocranium more than they impact the shape of the rostral part whereas the mass of the masseter correlates more with the shape of the rostral part of the cranium.

For the PCSA, the total PCSA of the jaw adductors explains roughly the same amount of variation in the complete shape of the cranium ($R^2 = 0.074$) or mandible ($R^2 = 0.078$). However, the PCSA of the jaw adductors better explains variation in the shape of the posterior part of the mandible (12%) than the shape of the posterior part of the cranium (7.4%). Procrustes ANOVAs performed on separate muscles show that the shape of the neurocranium is significantly better explained by the PCSA of the temporal and pterygoid muscles, whilst the rostral part of the cranium correlates more with the masseter. The coronoid process is explained mostly by variation in the temporal muscle.

The results of the covariation analyses between bone shape and masticatory muscles (digastric, masseter, temporal and pterygoids) are reported in Table 5. There are strong covariations between masticatory muscle mass and cranial shape. For the mandible, the covariations with muscle mass depend on the proxy used to scale muscle data. The only significant covariations are obtained between the mandibular ramus and scaled mass using mandible length or the centroid size of the mandibular ramus as a proxy of size for scaling. For the cranium, there is no clear difference in the amount of covariation between the different parts considered in the analyses.

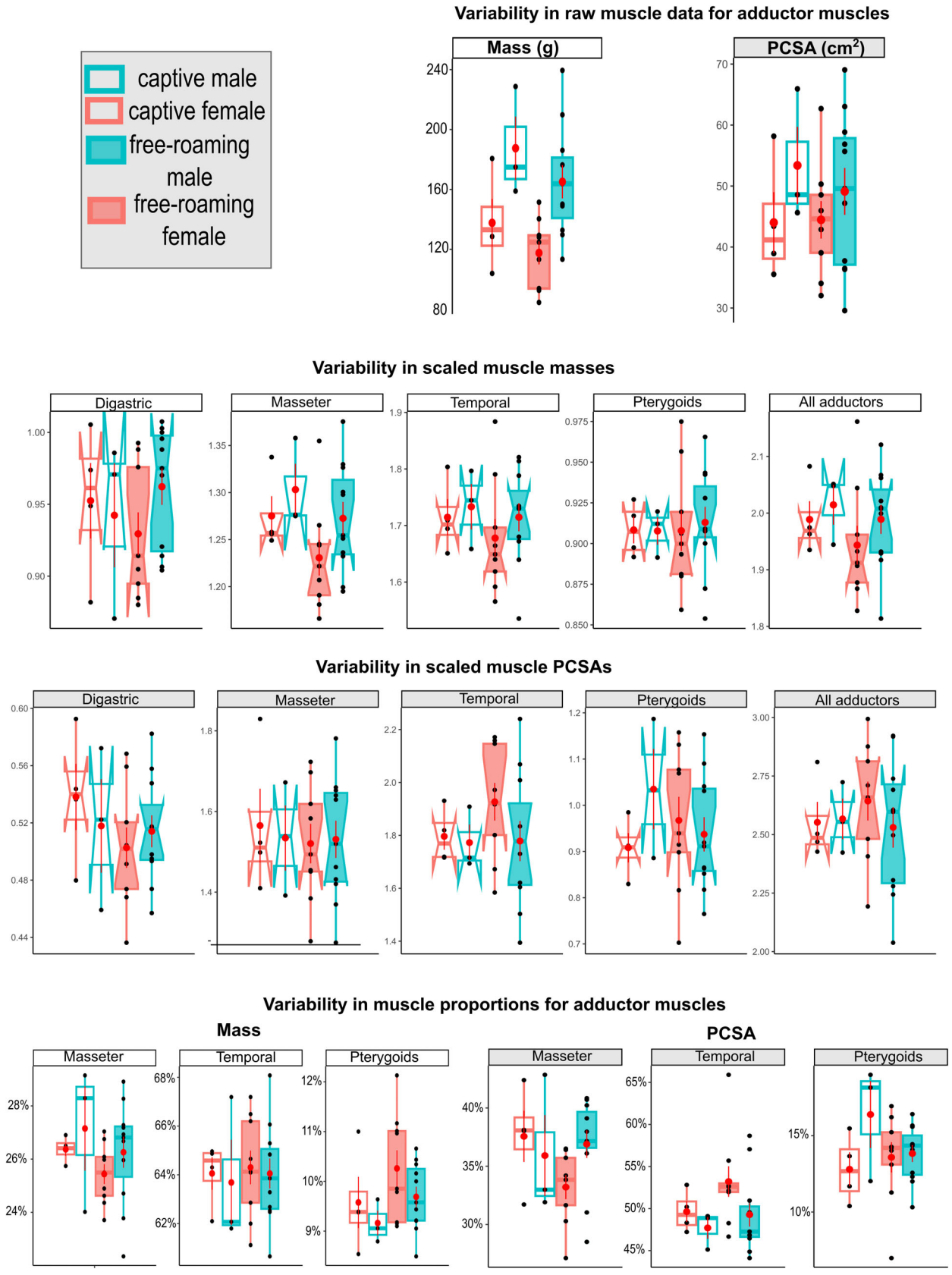

FIGURE 4 Variability in the raw and relative masses (g) and PCSAs (cm^2) and proportions to the total adductors mass or PCSA of the individual jaw muscles using the body mass as a proxy of size.

TABLE 4 Results of the Procrustes ANOVAs exploring the relationship between muscle mass or PCSA and cranial or mandibular shape.

Muscle data	Shape data	Digastric	Masseter	Temporal	Pterygoid	All adductors
$Mass^{1/3}$ scaled by $bodymass^{1/3}$	Cranium	$p = 0.6$	$p = 0.097$; $R^2 = 0.053$	$p = 0.013$; $R^2 = 0.07$	$p = 0.016$; $R^2 = 0.067$	$p = 0.014$; $R^2 = 0.069$
	Splanchnocranium	$p = 0.2$	$p = 0.01$; $R^2 = 0.076$	$p = 0.009$; $R^2 = 0.072$	$p = 0.039$; $R^2 = 0.063$	$p = 0.015$; $R^2 = 0.069$
	Neurocranium	$p = 0.4$	$p = 0.083$; $R^2 = 0.057$	$p = 0.008$; $R^2 = 0.075$	$p = 0.006$; $R^2 = 0.075$	$p = 0.016$; $R^2 = 0.074$
	Mandible	$p = 0.6$	$p = 0.3$	$p = 0.4$	$p = 0.9$	$p = 0.3$
	Mandibular body	$p = 0.5$	$p = 0.3$	$p = 0.4$	$p = 0.9$	$p = 0.3$
	Mandibular ramus	$p = 0.5$	$p = 0.3$	$p = 0.2$	$p = 0.9$	$p = 0.3$
$PCSA^{1/2}$ scaled by $bodymass^{1/3}$	Cranium	$p = 0.6$	$p = 0.3$	$p = 0.015$; $R^2 = 0.069$	$p = 0.011$; $R^2 = 0.076$	$p = 0.016$; $R^2 = 0.074$
	Splanchnocranium	$p = 0.2$	$p = 0.035$; $R^2 = 0.062$	$p = 0.047$; $R^2 = 0.062$	$p = 0.3$	$p = 0.015$; $R^2 = 0.069$
	Neurocranium	$p = 0.6$	$p = 0.3$	$p = 0.015$; $R^2 = 0.069$	$p = 0.011$; $R^2 = 0.076$	$p = 0.016$; $R^2 = 0.074$
	Mandible	$p = 0.11$	$p = 0.3$	$p = 0.002$; $R^2 = 0.086$	$p = 0.2$	$p = 0.007$; $R^2 = 0.078$
	Mandibular body	$p = 0.073$	$p = 0.15$	$p = 0.034$; $R^2 = 0.075$	$p = 0.049$; $R^2 = 0.073$	$p = 022$; $R^2 = 0.081$
	Mandibular ramus	$p = 0.026$	$p = 0.17$	$p = 0.001$; $R^2 = 0.11$	$p = 0.055$; $R^2 = 0.068$	$p = 0.001$; $R^2 = 0.12$

Note: The *p*-values (p) and coefficient of determination (R^2) are obtained after 1000 iterations.

There are strong covariations between masticatory muscle PCSA and both cranial shape and mandible shape. The covariations are approximately the same for the PCSA for both the complete cranium and complete mandible (there are slight variations depending on the proxy). The amount of covariation is roughly the same when considering the complete shape of the cranium or its different parts. However, for the mandibles, there are stronger covariations with the shape of the mandibular ramus than with that of the mandibular body.

We chose to represent the covariations between the shape of the complete cranium or mandible and the scaled PCSA (relative to cranial or mandible centroid size, respectively; Figure 5). For the first PLS axis, the level of covariation is strong and similar for both the complete cranium (0.77) and complete mandible (0.78). For the covariations based on cranial shape, the temporal muscle is the one that contributes the most and the masseter is the one that contributes the least. For the graph based on mandible shape, all the adductors contribute equally and the digastric contributes much less.

High relative PCSAs (on the right part of the scatterplot in Figure 5a and on the left side for Figure 5b) are associated with shorter skulls, with a higher and more rounded neurocranium. The zygomatic arches are larger and the sagittal crest is more pronounced (higher). Additionally, the post-orbital processes are more rostrally oriented. High relative PCSAs are also related to mandibles that are more curved ventrally and in the sagittal plane, with a more voluminous coronoid process, angular process and a deeper masseteric fossa.

4 | DISCUSSION

4.1 | Variability in architectural properties of the masticatory muscles

As in other carnivores, in the Tunisian street dogs, the temporalis is the largest muscle, representing 64.1 ± 2.0% of the total muscle mass of the adductors. Interestingly, it seems that the masseter and pterygoid muscles have a muscular architecture that optimizes muscle strength despite their lower relative muscle size. We found that the temporalis contributed around 50.4 ± 4.8% to the total PCSA, the masseter contributed around 26.2 ± 1.7% of the mass but 35.6 ± 4.2% to the total PCSA, and the pterygoids contributed around 9.8 ± 0.9% of the mass but 13.9 ± 2.6% of the total PCSA. These proportions match our previous data on dogs of different breeds [temporalis:

TABLE 5 Results of the covariation analyses between scaled jaw muscle mass or PCSA and cranial or mandible shape.

Muscle data	Factor used to scale muscle data	Shape data	Level of variability explained by PLS 1	*r*	*p*
$Mass^{1/3}$	$Bodymass^{1/3}$	Cranium	99%	0.77	0.017
		Splanchnocranium	99%	0.77	0.008
		Neurocranium	99%	0.72	0.011
		Mandible	79%	0.69	0.5
		Mandibular body	80%	0.61	0.4
		Mandibular ramus	78%	0.58	0.32
	Cranial length	Cranium	99%	0.77	0.017
		Splanchnocranium	99%	0.77	0.008
		Neurocranium	99%	0.72	0.011
	Cranial centroid size	Cranium	99%	0.77	0.017
	Splanchnocranium centroid size	Splanchnocranium	99%	0.77	0.008
	Neurocranium centroid size	Neurocranium	99%	0.72	0.011
	Mandible length	Mandible	90%	0.78	0.067
		Mandibular body	88%	0.68	0.26
		Mandibular ramus	91%	0.68	0.038
	Mandible centroid size	Mandible	91%	0.75	0.052
	Mandibular body centroid size	Mandibular body	90%	0.68	0.28
	Mandibular ramus centroid size	Mandibular ramus	90%	0.63	0.038
$PCSA^{1/2}$	$Bodymass^{1/3}$	Cranium	85%	0.77	0.031
		Splanchnocranium	89%	0.76	0.028
		Neurocranium	87%	0.74	0.032
		Mandible	72%	0.76	0.017
		Mandibular body	82%	0.64	0.013
		Mandibular ramus	83%	0.72	0.001
	Cranial length	Cranium	85%	0.77	0.031
		Splanchnocranium	89%	0.76	0.028
		Neurocranium	87%	0.74	0.032
	Cranial centroid size	Cranium	85%	0.77	0.031
	Splanchnocranium centroid size	Splanchnocranium	89%	0.76	0.028
	Neurocranium centroid size	Neurocranium	97%	0.75	0.032
	Mandible length	Mandible	75%	0.78	0.009
		Mandibular body	83%	0.66	0.011
		Mandibular ramus	86%	0.75	0.001
	Mandible centroid size	Mandible	75%	0.78	0.007
	Mandibular body centroid size	Mandibular body	81%	0.64	0.03
	Mandibular ramus centroid size	Mandibular ramus	87%	0.78	0.001

Note: *r* corresponds to the coefficient of covariation and *p* correspond to the *p*-value after 1000 permutations. Muscle data were scaled by considering the residuals of the regression between the $\log_{10}$ muscle data and the $\log_{10}$ of the centroid size of the corresponding bone.

64% of mass (min 55–max 71) and 50% (40–61) of PCSA; masseter: 27% (22–32) of the mass and 36% (29–46) of the PCSA; pterygoids: 9.6% (6–13) of mass and 14% (6–24) of the PCSA; Brassard, Merlin, Monchâtre-Leroy, et al., 2020]. This suggests that the overall morphology of the jaw adductor muscles is remarkably conserved among dogs, despite great morphological variation in cranial shape.

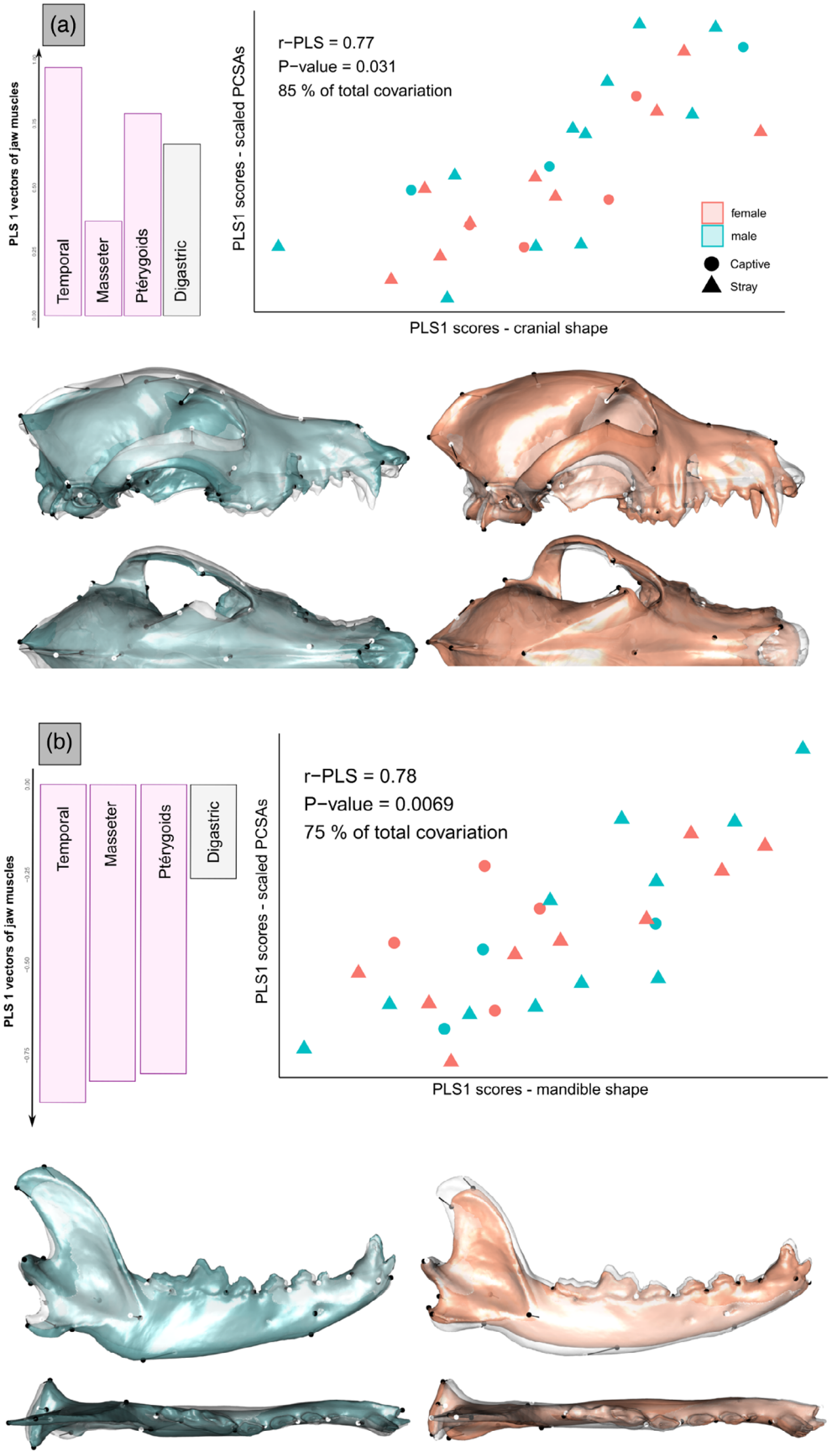

FIGURE 5 2-Block partial least square (2B-PLS) analyses between scaled jaw muscle PCSAs and (a) cranial or (b) mandibular shape in Tunisian street dogs. Shapes at the minimum and maximum of the PLS axis are illustrated. Illustrations represent deformations from the consensus to the extreme of the axis in lateral and dorsal views. Deformations were magnified by a factor three for the cranium. Different sexes are represented by different colors and different living status are represented by different shapes. The vectors of jaw muscles represent the contribution of the different muscles to the covariation axis. The digastric (in gray) is the only muscle that lowers the mandibles whilst the temporalis, masseter and pterygoids (in purple) are jaw elevators.

The very small part that the lateral pterygoid composes of the jaw adductors (0.47 ± 0.18% of the total mass) also matches previous studies on dogs of different breeds (0.66%; Brassard, Merlin, Monchâtre-Leroy, et al., 2020) and red foxes (0.77%; Brassard et al., 2021). This, combined with the fact that the muscle is attached very close to the joint, which makes it act more like a stabilizer of the mandible, explains why this muscle is often not dissected separately or is added to the medial pterygoid and treated as a single muscle.

4.2 | Scaling of muscle data

We found that the mass and PCSA of the digastric muscle, the jaw adductors as a whole, and all three of the jaw adductors muscle groups individually, scale isometrically to body mass. This is consistent with what has been previously demonstrated in Canidae (Penrose et al., 2016), primates (Cachel, 1984) and wild boar (Herrel et al., 2024). However, Penrose et al. (2016) focused only on the muscle masses of the jaw adductors and did not dissect the digastric muscle or record other architectural data necessary to calculate the PCSA.

4.3 | Sexual dimorphism in free-roaming street dogs

Whilst our sample sizes per sex in the free-roaming group were relatively modest, we found some significant differences in the jaw adductors between males and females. Females tend to have lower muscle masses relative to body mass for the digastric ($P = 0.06$) and the overall adductor muscles ($p = 0.11$; in particular the masseter and temporalis). However, we found that females tend to have greater relative PCSAs of the temporalis muscle ($p = 0.10$) and a temporalis muscle that contributes more to the total PCSA of the jaw adductors than males. If confirmed with a larger sample, these results would suggest that females develop some functional adaptations that optimize strength despite a smaller muscle and body size. This could be related to different predation or competitive behaviors between the two sexes. Conversely, males might exhibit adaptations that optimize size, potentially linked to differences in sexual behavior, communal pack dominance, or sexual selection. However, the total PCSA of the temporalis muscle is not necessarily completely representative of the force of this muscle or its contribution to bite force, as it does not take into account skull shape changes that could be biomechanically advantageous for bite force (and that could differ between sexes).

4.4 | Preliminary differences between lifestyles

The relative mass and PCSA of the temporalis muscle appear limited to lower values in the captive compared to the free-roaming dogs (Figure 4). However, this is only a preliminary observation given the small sample, and several other factors, including pregnancy or lactation status, body condition, tooth wear and overall health, should be taken into account to fully explain such differences. If confirmed, it would suggest that the change in lifestyle and diet may impact jaw muscle architecture. The literature documenting the impact of captivity on jaw muscles architecture is scarce (Herrel et al., 2024; Neaux et al., 2021), but none has focused on canids, so we have no other study to compare our results to.

4.5 | Relations between muscle and skull morphology

We found that muscle mass (i.e., volume) is more closely related to *size* (body mass, bone length, or centroid size) than muscle PCSA. This is not surprising considering that PCSA also depends on fascicle length and pennation angle, characteristics that are related not only to size but also to muscle function. The centroid sizes of the complete cranium and mandible are efficient for predicting muscle data. The size of the caudal parts of the cranium and mandible, which provide jaw muscle attachment areas, is more closely related to (and thus a better predictors of) the mass and PCSA of the jaw adductors. However, whilst in the skull the volume of the caudal part is a better predictor of muscle data than the rostral part, this is less clear for the mandible (the coefficients of determination are less different; Table 3). This suggests greater modularity in the cranium compared to the mandible, which could be explained by the fact that the mandible is more specialized towards mastication, whilst the cranium has additional functions such as protecting the brain and sensory organs. Additionally, the size of the cranium (more precisely the posterior part) is more closely related to adductor mass and PCSA than the size of the mandible (more precisely its caudal part).

Regarding *shape*, we found that muscle mass (i.e., volume) strongly contributes to explaining cranial shape but not mandible shape. However, muscle PCSA correlates with the shape of both bones. This difference could be explained by the fact that the cranium is subjected to important volume constraints compared to the mandible and that the area of insertion of the muscles is more significant on the cranium than on the mandible (Figure 2). Interestingly, we found that cranial and

mandible shape are more strongly driven by muscle PCSA than by muscle mass, contrary to previous results in dogs of different breeds (Brassard, Merlin, Guintard, Monchâtre-Leroy, Barrat, Bausmayer, et al., 2020a). This difference could be explained by the fact that here we focused on street dogs not artificially selected for aesthetic reasons (which may accentuate developmental constraints) but subjected to more natural constraints (allowing for functional adaptations) resulting in bone remodeling due to external forces exerted by the jaw muscles.

We found that the PCSA of the jaw adductors better explains variation in the shape of the posterior part of the mandible (12%) than the shape of the posterior part of the cranium (7.4%), which supports the idea that the mandible is a better predictor of muscle strength than the cranium (but not of muscle mass), but only if we consider the area of attachment of muscles. These results highlight the specialization of the mandible towards mastication and biting. This is in accordance with previous results on dogs of various breeds (for which muscle data explain less of the total variation in cranial shape than in mandibular shape; Brassard, Merlin, Guintard, Monchâtre-Leroy, Barrat, Callou, et al., 2020b). We further found that the shape of the neurocranium is significantly explained by the PCSA of the temporalis and pterygoid muscles, whilst the rostral part of the cranium correlates with the masseter, and the coronoid process is explained by the temporalis.

The covariation analyses performed on the PCSA data additionally led to a better coefficient of covariation for the cranium compared to the mandible, as found previously in dogs of different breeds (Brassard, Merlin, Guintard, Monchâtre-Leroy, Barrat, Callou, et al., 2020b). This could be due to the greater morphological diversity in the cranium compared to the mandible, which artificially increases the covariation. The visualizations provided by the 2B-PLS analyses revealed that strong jaw muscles are associated with shorter skulls, a higher and more rounded neurocranium, larger zygomatic arches, a more developed sagittal crest, and more rostrally oriented post-orbital processes. Moreover, the mandibles are more ventrally curved and curved in the sagittal plane, with a more voluminous coronoid process, angular process, and a deeper masseteric fossa.

The anatomical traits on the skull mainly correspond to the area of origin for the temporalis (see Figure 3). This may explain its greater contribution to the shape of the neurocranium compared to other muscles, according to the Procrustes ANOVAs. The area of origin of the masseter and digastric is very limited, which may explain the lower correlation rates obtained with these muscles. These findings suggest that the external shape of the cranium (especially the neurocranium) is driven by the necessity to accommodate the temporalis and, to a lesser extent, the other muscles. This has been suggested in Canidae by Penrose et al. (2016). As suggested by these authors, the major morphological adaptations (and more obvious ones) to increase the space on the skull for housing the temporalis are the widening of the zygomatic arches, the dorsoventral enlargement of the calvaria, and the more elevated sagittal crest. Other species display similar morphological patterns of accommodation, such as large species of primates (Ankel-Simons, 2007; Frost et al., 2003).

The anatomical traits on the mandible also mainly reflect the area of insertion of the temporalis muscle on the medial aspect and the dorsolateral top of the coronoid process (Figure 3). The masseter also shows a large insertion area and this may explain the variation observed in the depth of the masseteric fossa. The pterygoid muscle probably explains the variation observed in the angular process. The differences in the ventral curvature of the mandible might directly reflect variation in the digastric muscle, the only muscle lowering the mandible. Its importance is directly correlated to the importance of the jaw adductors. Thus, a more ventrally curved mandible reflects more strongly developed jaw adductors. We observe that most of the anatomical changes are located in the posterior part of the cranium and mandible. However, we also observe parallel variations, such as the width of the snout and the curvature of the mandible in the sagittal plane. These changes may reflect more global biomechanical adaptations than simply the impact of local load on the areas of insertion of the muscles. Our results directly link shape change in the cranium and mandible with the accommodation of the temporalis and suggest that the rostral and mandibular components are chiefly concerned with dietary specialization, whilst the cranial component is more strongly associated with muscle accommodation.

4.6 | Perspectives

Documenting the variability in muscle data and the relationship with shape data in street dogs is promising for comparisons not only with dogs of purebred breeds but also with dogs returned to the wild (dingoes) or they wild counterparts (wolf). This would allow us to decipher the impact of natural versus artificial selection on the jaw apparatus of dogs by exploring their morphofunctional adaptations in relation to their lifestyle or diet. Indeed, it is likely that wolves hunting in packs solicit differently their jaw muscles compared to dingoes eating carrion, street dogs feeding on garbage, and pet dogs feeding on

kibble. Unfortunately, no data on large samples are available so far rendering our understanding of the impact of artificial versus natural selection on the morpho-functional integration in the jaw apparatus limited. Moreover, documenting the relations between muscle and bone shape may help inform studies on the masticatory abilities of ancient specimens for which only bones are available.

AUTHOR CONTRIBUTIONS

Colline Brassard: Investigation; funding acquisition; writing – original draft; methodology; visualization; software; formal analysis; conceptualization; data curation; writing – review and editing. **Lobna Wertani:** Investigation; writing – review and editing. **Anthony Herrel:** Writing – original draft; writing – review and editing; funding acquisition; investigation. **Hassen Jerbi:** Data curation; supervision; resources; writing – review and editing; project administration.

ACKNOWLEDGMENTS

We thank the Fyssen Foundation for providing financial support. We thank the technical staff of the anatomy service of the veterinary school in Sidi Thabet for help in collecting and managing the cadavers (Omor Drissi, Tayeb Mejri and Noamen Zoubayr). We sincerely thank Anne Burrows and an anonymous reviewer for their constructive and insightful feedback on a previous version of the manuscript.

ORCID

Colline Brassard https://orcid.org/0000-0002-9789-2708
Anthony Herrel https://orcid.org/0000-0003-0991-4434

REFERENCES

Adams, D. C., & Collyer, M. L. (2016). On the comparison of the strength of morphological integration across morphometric datasets. *Evolution*, *70*, 2623–2631. https://doi.org/10.1111/evo.13045

Adams, D. C., & Collyer, M. L. (2017). Multivariate phylogenetic comparative methods: Evaluations, comparisons, and recommendations. *Systematic Biology*, *67*, 14–31.

Anderson, M. J. (2001). A new method for non-parametric multivariate analysis of variance. *Austral Ecology*, *26*, 32–46.

Anderson, M., & Braak, C. T. (2003). Permutation tests for multifactorial analysis of variance. *Journal of Statistical Computation and Simulation*, *73*, 85–113.

Anderson, R. A., Mcbrayer, L. D., & Herrel, A. (2008). Bite force in vertebrates: Opportunities and caveats for use of a nonpareil whole-animal performance measure. *Biological Journal of the Linnean Society*, *93*, 709–720. https://doi.org/10.1111/j.1095-8312.2007.00905.x

Ankel-Simons, F. (2007). Chapter 5 - Skull. In F. Ankel-Simons (Ed.), *Primate Anatomy (Third Edition)* (pp. 161–197). Academic Press. Available at: https://doi.org/10.1016/B978-012372576-9/50007-3.

Bourke, J., Wroe, S., Moreno, K., McHenry, C., & Clausen, P. (2008). Effects of gape and tooth position on bite force and skull stress in the dingo (Canis lupus dingo) using a 3 dimensional finite element approach. *PLoS One*, *3*, e2200. https://doi.org/10.1371/journal.pone.0002200

Brassard, C., Bălăşescu, A., Arbogast, R.-M., Forest, V., Bemilli, C., Boroneanţ, A., Convertini, F., Gandelin, M., Radu, V., Fleming, P. A., Guintard, C., Kreplins, T. L., Callou, C., Filippo, A., Tresset, A., Cornette, R., Herrel, A., & Bréhard, S. (2022). Unexpected morphological diversity in ancient dogs compared to modern relatives. *Proceedings of the Royal Society B: Biological Sciences*, *289*, 20220147. https://doi.org/10.1098/rspb.2022.0147

Brassard, C., Evin, A., Ameen, C., Curth, S., Michaud, M., Tamagnini, D., Dobney, K., Guintard, C., Porcier, S., & Jerbi, H. (2023). Wild or domestic? A 3D approach applied to crania to revisit the identification of mummified canids from ancient Egypt. *Archaeological and Anthropological Sciences*, *15*, 59. https://doi.org/10.1007/s12520-023-01760-1

Brassard, C., Forbes-Harper, J. L., Crawford, H. M., Stuart, J.-M., Warburton, N. M., Calver, M. C., Adams, P., Monchâtre-Leroy, E., Barrat, J., Lesellier, S., Guintard, C., Garès, H., Larralle, A., Triquet, R., Merlin, M., Cornette, R., Herrel, A., & Fleming, P. A. (2022). Morphological and functional divergence of the lower jaw between native and invasive red foxes. *Journal of Mammalian Evolution*, *29*, 335–352. https://doi.org/10.1007/s10914-021-09593-2

Brassard, C., Merlin, M., Guintard, C., Monchâtre-Leroy, E., Barrat, J., Bausmayer, N., Bausmayer, S., Bausmayer, A., Beyer, M., Varlet, A., Houssin, C., Callou, C., Cornette, R., & Herrel, A. (2020a). Bite force and its relationship to jaw shape in domestic dogs. *The Journal of Experimental Biology*, *223*, jeb224352. https://doi.org/10.1242/jeb.224352

Brassard, C., Merlin, M., Guintard, C., Monchâtre-Leroy, E., Barrat, J., Callou, C., Cornette, R., & Herrel, A. (2020b). Interrelations between the cranium, the mandible and muscle architecture in modern domestic dogs. *Evolutionary Biology*, *47*, 308–324. https://doi.org/10.1007/s11692-020-09515-9

Brassard, C., Merlin, M., Monchâtre-Leroy, E., Guintard, C., Barrat, J., Callou, C., Cornette, R., & Herrel, A. (2020). How does masticatory muscle architecture covary with mandibular shape in domestic dogs? *Evolutionary Biology*, *47*, 133–151. https://doi.org/10.1007/s11692-020-09499-6

Brassard, C., Merlin, M., Monchâtre-Leroy, E., Guintard, C., Barrat, J., Garès, H., Larralle, A., Triquet, R., Houssin, C., Callou, C., Cornette, R., & Herrel, A. (2021). Masticatory system integration in a commensal canid: Interrelationships between bones, muscles and bite force in the red fox. *The Journal of Experimental Biology*, *224*, jeb224394. https://doi.org/10.1242/jeb.224394

Cachel, S. (1984). Growth and allometry in primate masticatory muscles. *Archives of Oral Biology*, *29*, 287–293. https://doi.org/10.1016/0003-9969(84)90102-X

Christiansen, P., & Adolfssen, J. S. (2005). Bite forces, canine strength and skull allometry in carnivores (Mammalia, carnivora). *Journal of Zoology*, *266*, 133–151. https://doi.org/10.1017/S0952836905006643

Christiansen, P., & Wroe, S. (2007). Bite forces and evolutionary adaptations to feedinge ecology in carnivores. *Ecology*, *88*, 347–358. https://doi.org/10.1890/0012-9658(2007)88[347:BFAEAT]2.0.CO;2

Cignoni, P., Callieri, M., Corsini, M., Dellepiane, M., Ganovelli, F., & Ranzuglia, G. (2008). *MeshLab: An open-source*

mesh processing tool. The Eurographics Association. https://doi.org/10.2312/LocalChapterEvents/ItalChap/ItalianChapConf2008/129-136

Collyer, M. L., Sekora, D. J., & Adams, D. C. (2015). A method for analysis of phenotypic change for phenotypes described by high-dimensional data. *Heredity*, *115*, 357–365.

Damasceno, E. M., Hingst-Zaher, E., & Astúa, D. (2013). Bite force and encephalization in the Canidae (Mammalia: Carnivora). *Journal of Zoology*, *290*, 246–254. https://doi.org/10.1111/jzo.12030

Druzinsky, R. E., Doherty, A. H., & De Vree, F. L. (2011). Mammalian masticatory muscles: Homology, nomenclature, and diversification. *Integrative and Comparative Biology*, *51*, 224–234. https://doi.org/10.1093/icb/icr067

Dryden, I. L., & Mardia, K. V. (2016). *Statistical shape analysis: With applications in R*. John Wiley & Sons.

Ellis, J. L., Thomason, J. J., Kebreab, E., & France, J. (2008). Calibration of estimated biting forces in domestic canids: Comparison of post-mortem and in vivo measurements. *Journal of Anatomy*, *212*, 769–780. https://doi.org/10.1111/j.1469-7580.2008.00911.x

Ellis, J. L., Thomason, J., Kebreab, E., Zubair, K., & France, J. (2009). Cranial dimensions and forces of biting in the domestic dog. *Journal of Anatomy*, *214*, 362–373. https://doi.org/10.1111/j.1469-7580.2008.01042.x

Forbes-Harper, J. L., Crawford, H. M., Dundas, S. J., Warburton, N. M., Adams, P. J., Bateman, P. W., Calver, M. C., & Fleming, P. A. (2017). Diet and bite force in red foxes: Ontogenetic and sex differences in an invasive carnivore. *Journal of Zoology*, *303*, 54–63. https://doi.org/10.1111/jzo.12463

Frost, S. R., Marcus, L. F., Bookstein, F. L., Reddy, D. P., & Delson, E. (2003). Cranial allometry, phylogeography, and systematics of large-bodied papionins (Primates: Cercopithecinae) inferred from geometric morphometric analysis of landmark data. *The Anatomical Record*, *275A*, 1048–1072.

Goodall, C. (1991). Procrustes methods in the statistical analysis of shape. *Journal of the Royal Statistical Society: Series B: Methodological*, *53*, 285–321.

Grandjean, D. (2010). *The dog encyclopedia*. Aniwa Publishing.

Gunz, P., Mitteroecker, P., & Bookstein, F. L. (2005). Semilandmarks in three dimensions. In D. E. Slice (Ed.), *Modern morphometrics in physical anthropology, developments in primatology: Progress and prospects* (pp. 73–98). Springer US. https://doi.org/10.1007/0-387-27614-9_3

Hartstone-Rose, A., Dickinson, E., Deutsch, A. R., Worden, N., & Hirschkorn, G. A. (2022). Masticatory muscle architectural correlates of dietary diversity in Canidae, Ursidae, and across the order carnivora. *The Anatomical Record*, *305*, 477–497. https://doi.org/10.1002/ar.24748

Hartstone-Rose, A., Perry, J. M. G., & Morrow, C. J. (2012). Bite force estimation and the fiber architecture of felid masticatory muscles. *The Anatomical Record*, *295*, 1336–1351. https://doi.org/10.1002/ar.22518

Haxton, H. A. (1944). Absolute muscle force in the ankle flexors of man. *The Journal of Physiology*, *103*, 267–273.

Herrel, A., Locatelli, Y., Ortiz, K., Theil, J.-C., Cornette, R., & Cucchi, T. (2024). Cranial muscle architecture in wild boar: Does captivity drive ontogenetic trajectories? *Journal of Morphology*, *285*, e21676. https://doi.org/10.1002/jmor.21676

Ito, K., & Endo, H. (2016). Compartive study of physiological cross-sectional area of masticatory muscles among species of carnivora. *Mammal Study*, *41*, 181–190. https://doi.org/10.3106/041.041.0403

Ito, K., & Endo, H. (2019). The effect of the masticatory muscle physiological cross-sectional area on the structure of the temporomandibular joint in carnivora. *The Journal of Veterinary Medical Science*, *81*, 389–396. https://doi.org/10.1292/jvms.18-0611

Ito, K., Kubo, M. O., Kodera, R., Takeda, S.-I., & Endo, H. (2024). Quantitative assessment of masticatory muscles based on skull muscle attachment areas in carnivora. *The Anatomical Record*, 1–27.

Kilmer, J. T., & Rodríguez, R. L. (2017). Ordinary least squares regression is indicated for studies of allometry. *Journal of Evolutionary Biology*, *30*, 4–12. https://doi.org/10.1111/jeb.12986

Kim, S. E., Arzi, B., Garcia, T. C., & Verstraete, F. J. M. (2018). Bite forces and their measurement in dogs and cats. *Frontiers in Veterinary Science*, *5*, 76. https://doi.org/10.3389/fvets.2018.00076

Klingenberg, C. P. (2013). Visualizations in geometric morphometrics: How to read and how to make graphs showing shape changes. *Hystrix, the Italian Journal of Mammalogy*, *24*, 15–24. https://doi.org/10.4404/hystrix-24.1-7691

Klingenberg, C. P., Barluenga, M., & Meyer, A. (2002). Shape analysis of symmetric structures: Quantifying variation among individuals and asymmetry. *Evolution*, *56*, 1909–1920. https://doi.org/10.1111/j.0014-3820.2002.tb00117.x

Law, C. J., & Mehta, R. S. (2019). Dry versus wet and gross: Comparisons between the dry skull method and gross dissection in estimations of jaw muscle cross-sectional area and bite forces in sea otters. *Journal of Morphology*, *280*, 1706–1713. https://doi.org/10.1002/jmor.21061

Méndez, J. V., & Keys, A. (1960). Density and composition of mammalian muscle. *Metabolism-Clinical and Experimental*, *9*, 184–188.

Neaux, D., Blanc, B., Ortiz, K., Locatelli, Y., Laurens, F., Baly, I., Callou, C., Lecompte, F., Cornette, R., & Sansalone, G. (2021). How changes in functional demands associated with captivity affect the skull shape of a wild boar (Sus scrofa). *Evolutionary Biology*, *48*, 27–40.

Penrose, F., Cox, P., Kemp, G., & Jeffery, N. (2020). Functional morphology of the jaw adductor muscles in the Canidae. *Anatomical Record (Hoboken, NJ: 2007)*, *303*(11), 2878–2903. https://doi.org/10.1002/ar.24391

Penrose, F., Kemp, G. J., & Jeffery, N. (2016). Scaling and accommodation of jaw adductor muscles in Canidae. *The Anatomical Record*, *299*, 951–966. https://doi.org/10.1002/ar.23355

R Core Team. (2021). R: A language and environment for statistical computing. R Foundation for Statistical Computing. https://www.R-project.org/.

Rohlf, F. J., & Corti, M. (2000). Use of two-block partial least-squares to study covariation in shape. *Systematic Biology*, *49*, 740–753. https://doi.org/10.1080/106351500750049806

Ruiz, J. V., Ferreira, G. S., Lautenschlager, S., de Castro, M. C., & Montefeltro, F. C. (2023). Different, but the same: Inferring the hunting behaviour of the hypercarnivorous bush dog (Speothos venaticus) through finite element analysis. *Journal of Anatomy*, *242*, 553–567. https://doi.org/10.1111/joa.13804

Ström, D., Holm, S., Clemensson, E., Haraldson, T., & Carlsson, G. E. (1988). Gross anatomy of the craniomandibular joint and masticatory muscles of the dog. *Archives of Oral Biology*, *33*, 597–604. https://doi.org/10.1016/0003-9969(88)90135-5

Thomason, J. J. (1991). Cranial strength in relation to estimated biting forces in some mammals. *Canadian Journal of Zoology*, *69*, 2326–2333. https://doi.org/10.1139/z91-327

Tomo, S., Hirakawa, T., Nakajima, K., Tomo, I., & Kobayashi, S. (1993). Morphological classification of the masticatory muscles in dogs based on their innervation. *Annals of Anatomy – Anatomischer Anzeiger*, *175*, 373–380. https://doi.org/10.1016/S0940-9602(11)80047-6

Turnbull, W. D. (1970). Mammalian masticatory apparatus. *Fieldiana: Geology*, *18*, 149–356.

United Kennel Club. 2022. Breed standards: Atlas mountain dog | United Kennel Club (UKC) https://www.ukcdogs.com/atlas-mountain-dog. Accessed July 25, 2024.

Wiley, D. F., Amenta, N., Alcantara, D. A., Ghosh, D., Kil, Y. J., Delson, E., Harcourt-Smith, W., Rohlf, F. J., John, K. S., & Hamann, B. (2005). Evolutionary morphing, in: VIS 05. IEEE visualization, 2005. Presented at the VIS 05. *IEEE Visualization*, *2005*, 431–438. https://doi.org/10.1109/VISUAL.2005.1532826

Wroe, S., McHenry, C., & Thomason, J. (2005). Bite club: Comparative bite force in big biting mammals and the prediction of predatory behaviour in fossil taxa. *Proceedings of the Royal Society B: Biological Sciences*, *272*, 619–625. https://doi.org/10.1098/rspb.2004.2986

Wroe, S., & Milne, N. (2007). Convergence and remarkably consistent constraint in the evolution of carnivore skull shape. *Evolution: International Journal of Organic Evolution*, *61*, 1251–1260.

SUPPORTING INFORMATION

Additional supporting information can be found online in the Supporting Information section at the end of this article.

How to cite this article: Brassard, C., Wertani, L., Herrel, A., & Jerbi, H. (2025). Variability of jaw muscles in Tunisian street dogs and adaptation to skull shape. *The Anatomical Record*, 1–20. https://doi.org/10.1002/ar.25638